national accelerator laboratory

TM-199
2257

SOME CONSIDERATIONS ON A HIGH INTENSITY, HIGH ENERGY, NEGATIVE HYPERON BEAM AT NAL

J. Sandweiss
Yale University

and

O. Overseth
University of Michigan

January 1970

I. GENERAL

This report summarizes some thoughts on an intense, high-energy Y^- beam for the 200-BeV accelerator. This work should be regarded as complementary to SS - 20[1] which considers a low-intensity beam produced via the diffraction scattered proton beam of $\sim 10^{10}$ protons per pulse.

Whereas the beam proposed in SS - 20 is especially designed for flux measurement, the beam suggested here is meant to be useful for a large class of possible experiments. In this respect, it is worth noting that many of these ideas were developed in a detailed experimental design of a high energy Y^- beam for the Brookhaven AGS by the Yale group. The AGS Y^- experiment is scheduled to be carried out in the coming year and will provide an interesting test of the approach. We note that the AGS experiment will provide flux measurements of Σ^-, Ξ^-, and Ω^-

at ~ 30 BeV bombarding energy. The subsequent prediction of the fluxes at 200 BeV should be on a much firmer footing than is presently possible.

Since time does not permit the same type of detailed study for the 200-BeV case as was carried out for the 30-BeV experiment, we shall often attempt to relate the 30- and 200-BeV setups as much as possible, and to proceed by using a comparative technique.

Our basic approach is to use a short, unfocused channel which gives high intensity because of its low decay loss and large momentum bite, despite a rather modest solid angle.

A central feature in our approach is the intention to measure the position and angle of the hyperon with high accuracy as it emerges from the shield, before it interacts or decays. With proportional wire spark chambers (Charpak chambers) it appears eminently possible to stand fluxes of $\sim 10^8$ particles per second. Since we anticipate Σ^-/π^- ratios in the beam (after the shield) of ~ 1/10, this implies that if the proton flux were available, we could utilize Σ^- rates of $\sim 10^7$/pulse. The precise measurement of position and angle of the exiting hyperon is essential as it allows the wide momentum bite and at the same time provides the precise resolution required for event identification, etc.

II. CONSIDERATIONS RELATING TO THE NEED FOR HIGH INTENSITY

We take this opportunity to point out that there are rather general arguments pointing to the conclusion that for a large class of experiments

the hyperon beams at NAL will need higher intensity than would be needed for AGS or Serpukhov energies.

In the case of the strong interactions of the hyperons, the higher NAL energy will make larger momentum transfers kinematically possible. However, the cross section traditionally decreases with increasing momentum transfer so that higher intensity will be needed to exploit the new region which the NAL energy makes kinematically possible.

In the case of the decay studies, one can anticipate that work at NAL will concentrate on the rarer decay modes. One example might be the study of muonic decays (e.g., $\Xi^- \rightarrow \Lambda^o + \mu^- + \nu$) where the higher NAL beam energy allows a cleaner separation between pions and muons with the interaction technique.

Finally, one can anticipate the use of tertiary hyperon beams, e.g., Λ^o's from Ξ^- decay would have well-defined momentum and polarization properties. These would be difficult, if not impossible, to obtain in any other way. Clearly, the use of tertiary beams will require the highest primary intensity.

III. BEAM DESIGN

The general layout of the beams considered here is illustrated in Fig. 1, which shows a simple unfocused magnetic channel. The significant parameters of the design are:

1. the thickness of the hadron shield L,
2. the spatial and magnetic geometry of the channel,
3. the separation h of the magnet coils.

In the following, we discuss briefly the considerations relating to the choice of these parameters and make tentative choices for the purposes of evaluating a specific beam in Section IV.

It may be useful to comment briefly at this point on the choice of an unfocused rather than a focused channel. The principal disadvantage, aside from complexity, of a focused channel is the additional length required which results in flux loss due to decay. The increased solid angle of the focused channel is also somewhat offset by the greater momentum bite of the unfocused channel at least as compared with most simple quadrupole arrangements. In this discussion, we are assuming an iron magnet. The use of superconducting magnets present serious problems of "trapped" muon background as will be discussed in the section of coil spacing. It may well be, however, that ingenious use of supermagnets offers substantial advantages, but the work on this subject is yet to be done.

If one limits oneself to iron magnets and agrees to measure the position and direction of the hyperon before it decays, the unfocused channel is superior.

Hadron Shield Thickness

We take the point of view that if we reduce the number of neutrons exiting the shield to a negligible number, we shall be adequately shielded with respect to hadrons. In these calculations we neglect the effect of the magnetic channel which will have a width small compared to a neutron mean free path. Nevertheless, this is a point which certainly deserves further detailed study.

To estimate the allowed number of neutrons, we assume that the experimental apparatus will use spark chambers with resolving (memory) time of $\sim 10^{-6}$ sec and that every neutron is the potential source of a track--a somewhat conservative estimate. If we further adopt the criterion of not more than one (neutron induced) background track per event and take a spill time of 1 sec we find an acceptable upper limit to the neutron flux of 10^6 neutrons per pulse. We further make the conservative assumption that the spark chambers are in "bad" geometry, i.e., a neutron exiting the shield at any lateral displacement will strike one of the spark chambers. We thus take our limit to apply to the total number of neutrons exiting the shield. Finally, to make some allowance for the beam hole, the charged particle background, and the errors in estimating the neutron rates, we take our criteria an order of magnitude lower.

We thus take the criterion for the hadron shield as follows: total number of neutrons exiting the shield $\leq 10^5$ per pulse.

We estimate the neutron background according to the methods outlined in the 1965 200-BeV Accelerator Design Study.[2] The number of neutrons N(Z), exiting a shield of thickness Z, bombarded by $N_p(0)$ 200-BeV proton is given as:

$$N(Z) = N_p(0) B_N e^{-Z/\lambda}. \qquad (1)$$

If we consider all neutrons of energy greater than 0.1 MeV, and take the mean free path λ for the case of bad geometry, we find:[2]

$$B_N = 1490, \quad \lambda = 160 \text{ g/cm}^2.$$

Assuming 10^{13} protons per pulse as the incident intensity, we see that we need:

$$\frac{N_p(0)}{N(Z)} \geq 10^8.$$

For a steel shield ($\rho = 7.87$ g/cm^3) this gives $L \geq 5.23$ meters. For the purposes of future discussion, we choose $L = 6$ meters. Rounding upwards gives some additional safety factor, costs little in decay and solid angle and helps in the momentum analysis.

The Channel Field "B"--Momentum Bite and Resolution

Clearly, one would like to make the magnetic field as large as possible. Since we are considering iron magnets, we take as a practical maximum a peak field of 30 kG. We shall show that with reasonable assumptions on target size and spark-chamber measuring position, 30 kG indeed provides adequate momentum analysis.

Figure 2 shows the geometry of the trajectories in the magnetic channel in the bending plane (presumably, the horizontal plane). In the small angle approximation, the differential equation governing the trajectories is:

$$\frac{d^2 g}{d\chi^2} = \frac{1}{\rho} - \frac{1}{\rho_0}, \tag{2}$$

where the radius of curvature of trajectory is ρ and the radius of curvature for the central momentum is ρ_0. For 30 kG field we have:

$$\rho \text{ (meters)} = 1.111 \text{ p (BeV/c)} \tag{3}$$

Integrating equation (2) and letting $C = \frac{1}{\rho} - \frac{1}{\rho_0}$:

$$\frac{dy}{d\chi} = C\chi + \theta_0 \tag{4}$$

$$y(x) = 1/2\, C\chi^2 + \theta_0 \chi + y(0). \tag{5}$$

In Fig. 2 and in this analysis, we have replaced the collimator with two "equivalent" slits at L and at L/2. Although the actual collimator would certainly extend throughout most of L, and be carefully shaped to minimize slit scattering, the two-slit approximation will show all the general features of the transmitted beam and is sufficiently accurate for our present purposes.

To analyze the precision of momentum measurement, we solve equations 4, 5 for C in terms of the angle θ_L and position y_L at $\chi = L$:

$$C = \frac{2}{L^2} (\theta_L + y_0 - y_2).$$

From the definition of C we have

$$\frac{|\Delta p|}{p} = 1.111\, p\ |\Delta C|$$

Neglecting correlations in the measurement of θ_L and y_L we thus find:

$$\frac{\Delta p}{p} = \frac{2.222p}{L^2}\sqrt{(L\Delta\theta_L)^2 + (\Delta y_0)^2 + (\Delta y_L)^2}\ . \qquad (6)$$

We assume a position measurement error of 0.1 mm and a lever arm of 1 meter for measurement of θ_L. This seems reasonable since even for momenta as low as 100 BeV/c the Σ^- decay length is ~4 meters. The error Δy_0 is essentially the 1/2 width of the target. Thus, for the following choices of parameters

$$\Delta\theta = 10^{-4}$$

$$\Delta y_0 = 5 \times 10^{-4} \text{ meters}$$

$$\Delta y = 10^{-4} \text{ meters}$$

$$L = 6 \text{ meters}$$

we have

$$\frac{\Delta p}{p}\ (\%) = 0.486\ \frac{p(\text{BeV/c})}{100}\ . \qquad (7)$$

We see that we may expect $\Delta p/p$ of 0.5% to 1% between 100 BeV/c and 200 BeV/c.

The errors due to target size and to θ_L measurement are nearly equal so for experiments which require better $\Delta p/p$ of the beam it would be necessary to decrease the target diameter as well as to increase the precision of θ_L measurement.

We now estimate the momentum interval transmitted. The momentum of a ray which leaves the target at y_0, passes $\chi = L/2$ at $y_{L/2}$ and passes $\chi = L$ at y_L is easily shown to be given by:

$$\frac{\Delta p}{p} = \frac{4.444p}{L^2} \left(y_L + y_0 - 2y_{L/2} \right) , \tag{8}$$

where p is in BeV/c and all distances are in meters. We make the approximation that the effective momentum interval for flux estimates is 1/2 the total interval transmitted from the center of the target. This is essentially a "small target" approximation which will be valid here to within ~10%. Finally, we assume that the slit at $\chi = L/2$ is matched to the slit at $\chi = L$ for the central momentum, i.e., $w_E = w_H/2$ (see Fig. 1).

We thus find for the effective momentum interval:

$$\left(\frac{\Delta p}{p} \right)_{eff} = \frac{2.222pw_H}{L^2} . \tag{9}$$

Taking L = 6 meters as before and for example choosing $w_H = 1$ cm gives:

$$\left(\frac{\Delta p}{p} \right)_{eff} (\%) = 6.19 \left[\frac{p(\text{BeV/c})}{100} \right] . \tag{10}$$

This illustrates the feature of the unfocused channel discussed previously. Namely, the simple channel offers high momentum transmission while at the same time allowing much more precise momentum definition of individual events.

One point is perhaps worth noting, namely, these formulas assume that at each value of p considered, B is kept constant (and equal to 30 kG). At each value of p, then, the channel would have a different curvature. In other words, this is a design optimized for each p considered. Once a value of p CENTRAL is chosen and the channel curvature fixed, the formulas would have to be modified to take into account that to transmit different momenta, the magnetic field must change.

Separation of Magnet Coils--Muon Background

The coils and the associated return flux have the property of "channeling" the penetrating muons. Detailed calculations for the AGS experiment show that this is a very important effect and that a large muon background exits the shield in the vicinity of the coils.

For this reason, the coil spacing (h on Fig. 1) must be large enough so that the muon background misses the apparatus. However, if we keep the same coil spacing at NAL as we used at the AGS, the muon background to the experiment may well be negligible at NAL. This is partly because the average decay length of the secondary pions increases with energy while the interaction length remains constant. Secondly, the NAL experiment apparatus will be narrower in lateral extent than the AGS apparatus and thus the NAL experiment will be further away from the coils and the muons. Clearly, this problem requires careful, detailed study for any actual hyperon experiment planned for NAL.

IV. PERFORMANCE OF A SPECIFIC BEAM -Y^- FLUX ESTIMATES

Reference 1 gives an estimate of Y^- yields from 200-GeV protons. We give here an estimate of a somewhat different character and as it turns out, one which is considerably more pessimistic than that given in Ref. 1.

The principle physics difference is that we consider the major intermediate states to be S = -1 baryon resonances and Ref. 1 considers the dominant source to be S = 0 baryon states which decay into strange particle systems. The results are qualitatively the same as far as energy spectra of the hyperons are concerned but Ref. 1 predicts fluxes about a factor of 30 higher than our method. At the present time, not enough data exists to decide which method (if any) is correct. However, it seems quite reasonable to regard our estimates as somewhat in the nature of lower limits to the hyperon yields. As noted earlier, when the AGS experiment is carried out, hyperon flux estimates could be made in a much more reliable fashion.

Our estimate of Σ^- production is as follows. From 20-30 GeV data and cosmic-ray data, we assume that 10% of all proton interactions produce negative strangeness baryon systems (essentially the K^+ to K^- excess attributed to associated production).

At the time of writing three S = -1 baryon states which can have charge = + 1 have decays which are clearly known, Σ^-, $Y_1^*(1385)$, $Y_1^*(1765)$. Approximately twice as many S = -1 baryon resonances are

known to exist. It is not known which are produced in proton-nucleon collisions nor are the decay chains known for the newer higher mass states. We make the conservative assumption that only the $Y_1^*(1765)$ contributes to Σ^- productions and that it is produced in 1/6 of the interactions which produce S = -1 baryon systems. The chain is as follows:

$$p \rightarrow Y_1^{*+}(1765)$$
$$\hookrightarrow Y_0^*(1520) + \pi^+$$
$$\hookrightarrow \Sigma^- + \pi^+ .$$

Recalling that we are interested in high energy (lab) Σ^-, hence those which are produced in the forward hemisphere in the CM and using the known branching ratios, we write for f_{Σ^-} (the fraction of all proton interactions which produce a Σ^-)

$$f_{\Sigma^-} = \underset{\substack{\text{Fraction} \\ \rightarrow S = -1 \text{ Systems}}}{\frac{1}{10}} \times \underset{\substack{Y_1^*(1765) \\ \text{All } S = -1}}{\frac{1}{6}} \times \underset{\substack{Y_1^*(1765) \\ \rightarrow Y_0^*(1520) \\ \text{Branching fraction}}}{\frac{1}{10}} \times \underset{\substack{Y_0^*(1520) \\ \rightarrow \Sigma^-\pi^+ \text{ B.F.}}}{\frac{1}{5}} \times \underset{\substack{\text{Forward} \\ \text{in CM} \\ \text{fraction}}}{\frac{1}{2}}$$

$$\therefore f_{\Sigma^-} = \frac{1}{6000} .$$

We now assume the fast Σ^- are distributed in momentum and angle as the fast inelastic protons are distributed. We estimate $d^2N/d\Omega\, dp$ for the inelastic protons starting with the data of Ref. 3 as

follows. We assume that the transverse momentum spectrum and the inelasticity do not change with incident energy and that the longitudinal momentum spectrum maintains the same shape. We thus write:

$$\left.\frac{d^2\sigma}{d\Omega\, dp}\ (p)\right|_{200} = \left(\frac{200}{30}\right)^2 \times \left(\frac{30}{200}\right) \left.\frac{d^2\sigma}{d\Omega\, dp}\left(\frac{30}{200}\,p\right)\right|_{30}$$

solid angle compression factor

energy scale expansion factor

$$\left.\frac{d^2\sigma}{d\Omega\, dp}\ (p)\right|_{200} = \frac{200}{30} \left.\frac{d^2\sigma}{d\Omega\, dp}\left(\frac{30}{200}\,p\right)\right|_{30}.$$

To relate the cross section to the number per interaction, we make the conservative assumption that one (1) fast proton (inelastic) is produced per interaction (1 is certainly an upper limit and using it probably underestimates the Σ^- flux). Whence we may write:

$$\left.\frac{d^2N}{d\Omega\, dp}\ (\Sigma^- \text{ of mom. } p)\right|_{200} = \frac{1}{900} \left.\frac{d^2N}{d\Omega\, dp}\ \begin{pmatrix}\text{protons of mom. of} \\ \frac{30}{200}\ p\end{pmatrix}\right|_{30}. \qquad (11)$$

Figure 3 shows the results of Eq. (11) and also gives the π^- yield (from Be) as given in the compilation of Awschalom and White [4]. We estimate the Ξ^- and Ω^- yields very crudely by the "rule-of-thumb":

$$\frac{d^2N}{d\Omega\, dp}\ (\Xi^-) = \frac{1}{30}\ \frac{d^2N}{d\Omega\, dp}\ (\Sigma^-) \qquad (12)$$

and

$$\frac{d^2N}{d\Omega\, dp}\ (\Omega^-) = \frac{1}{900}\ \frac{d^2N}{d\Omega\, dp}\ (\Sigma^-)\,. \qquad (13)$$

For completeness we record the decay lengths we have used (evaluated from the most recent Rosenfeld table):

$$\text{Mean decay path } \Sigma^- \text{ (meters)} = 4.109 \frac{p(\text{GeV/c})}{100}$$

$$\text{Mean decay path } \Xi^- \text{ (meters)} = 3.769 \frac{p(\text{GeV/c})}{100}$$

$$\text{Mean decay path } \Omega^- \text{ (meters)} = 2.332 \frac{p(\text{GeV/c})}{100} .$$

To illustrate the yields for a "typical" beam, we choose according to the arguments of the previous section the following parameters:

L = 6 (shield) + 1 (measurement of Y^-) = 7 meters

$w_H = w_V$ = 1 cm

w_E = 0.5 cm

B = 30 kG

p_0 = 160 GeV/c.

Figure 4 shows the π^-, Σ^-, Ξ^-, and Ω^- yields for such a beam with the preceding assumptions. We see that with 10^{12} interacting protons we may expect Σ^- fluxes in excess of 10^5 and pion background fluxes of $\lesssim 10^7$ for secondary beam momenta in the vicinity of 160 GeV/c. Although the Ω^- (and Ξ^-) rates are more speculative, it is interesting to note that several hundred Ω^- and some tens of thousands Ξ^- are predicted for 10^{12} interacting protons.

REFERENCES

[1]D. Berley, G. Bingham, and G. Conforto, A Hyperon Beam in Target-Area 2, National Accelerator Laboratory 1969 Summer Study Report SS-20, Vol. I, p. 63.

[2]Section XII, 200-BeV Accelerator Design Study, Lawrence Radiation Laboratory, UCRL-16830, Vol. I.

[3]E. W. Anderson et al., Phys. Rev. Letters 16, 855 (1966); F. Turkot, private communication.

[4]M. Awschalom and T. White, Secondary Particle Production at 200 GeV, National Accelerator Laboratory FN-191, June 9, 1969.

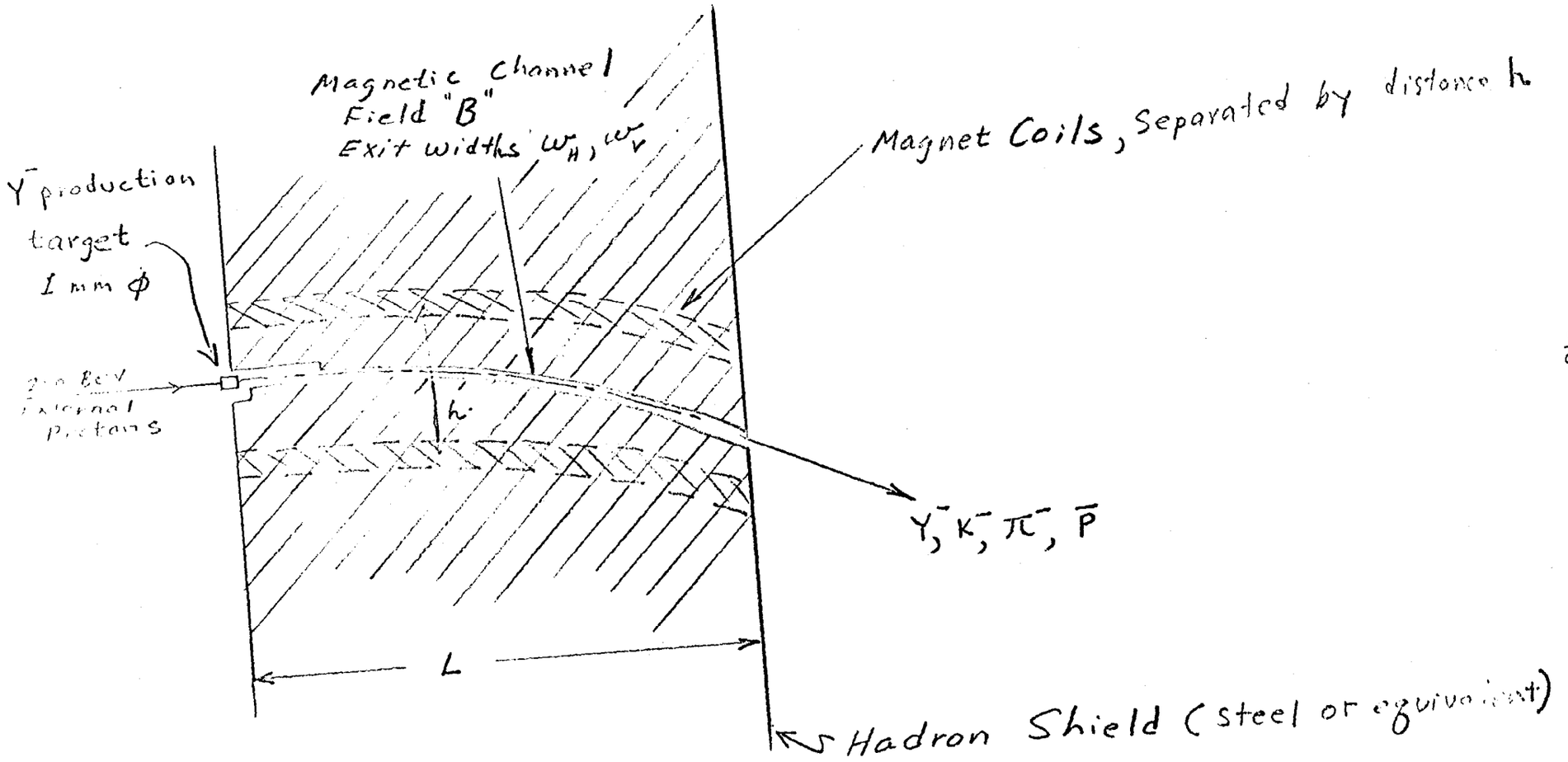

FIG 1

Schematic Design of Unfocussed Hyperon Beam

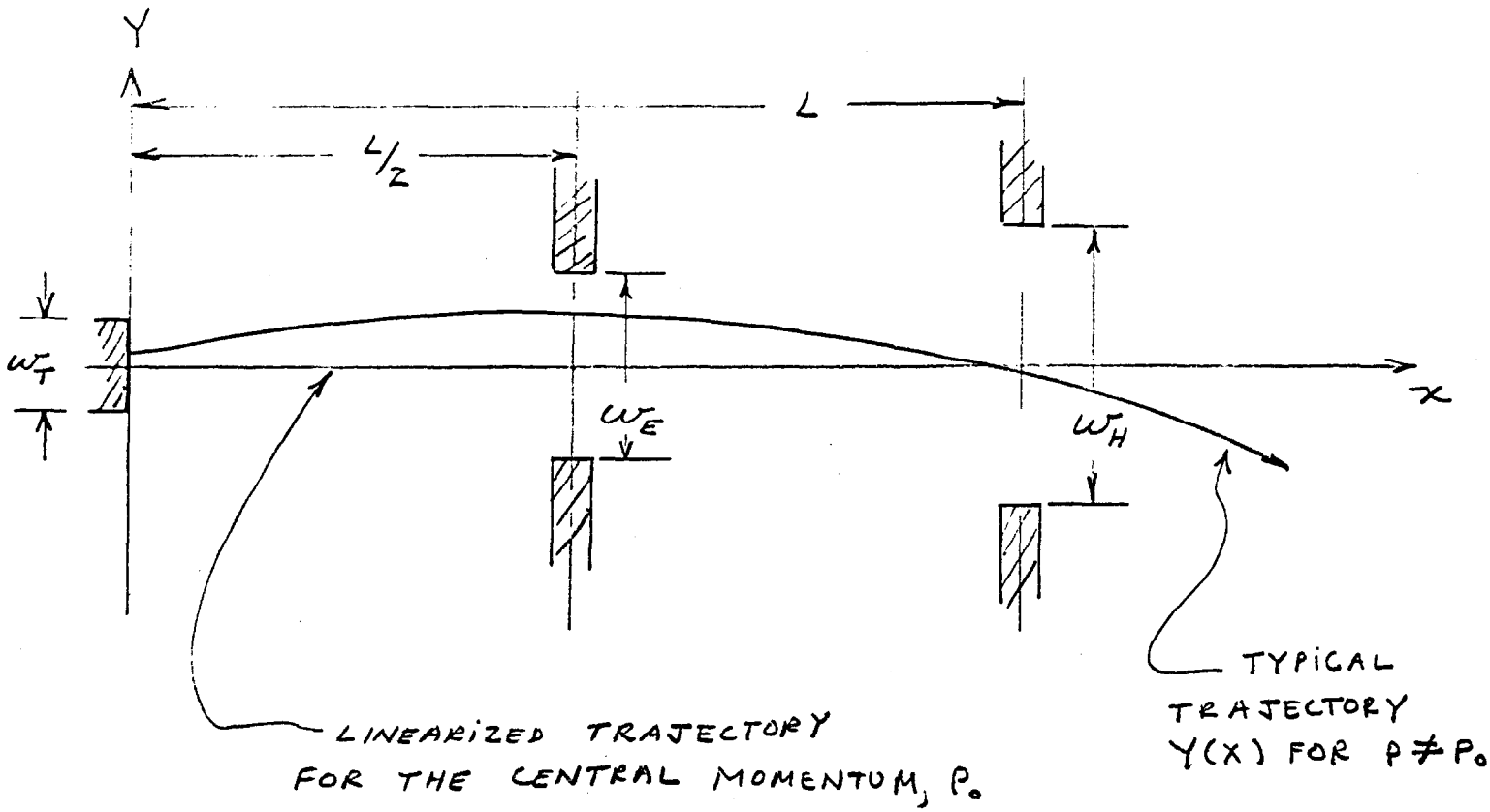

FIG 2 GEOMETRY OF THE MAGNETIC CHANNEL

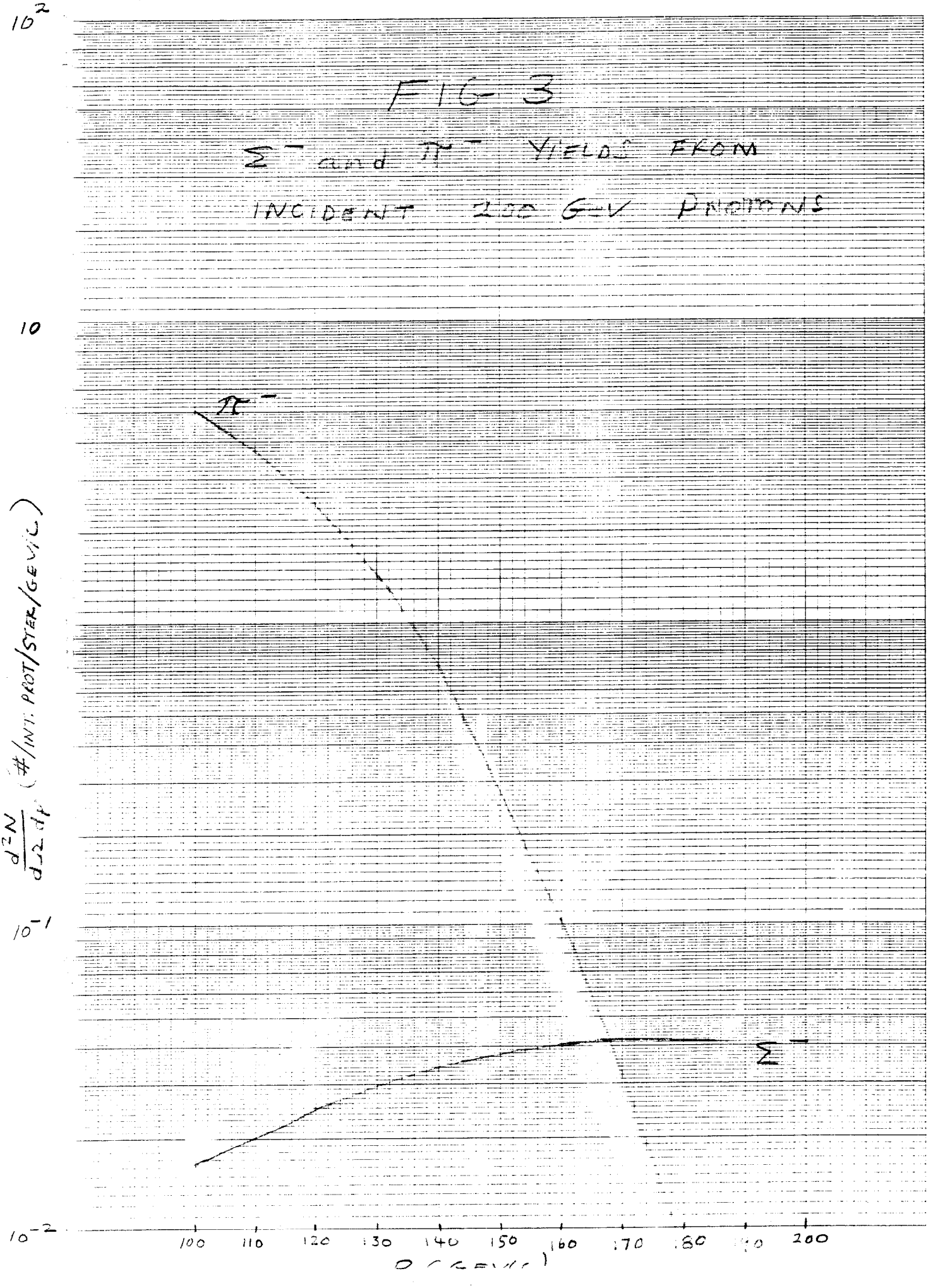
FIG 3
Σ⁻ and π⁻ YIELDS FROM
INCIDENT 200 GeV PROTONS
10²
10
10⁻¹
10⁻²
π⁻
Σ⁻
d²N/dΩ dp (#/INT. PROT/STER/GEV/c)
100
110
120
130
140
150
160
170
180
190
200
P (GeV/c)

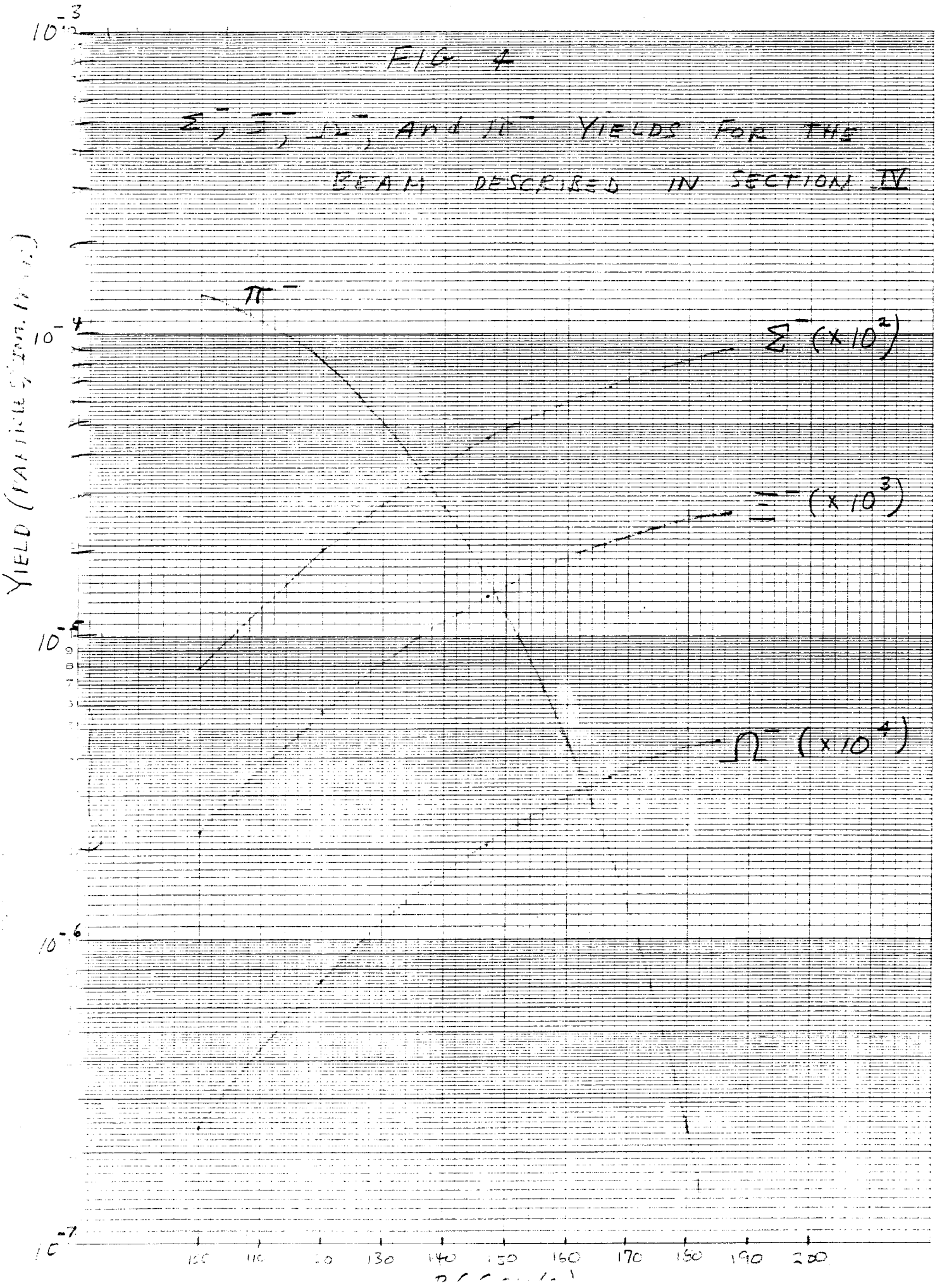
FIG 4
Σ^-, Ξ^-, Ω^-, And π^- YIELDS FOR THE
BEAM DESCRIBED IN SECTION IV
YIELD (PARTICLES / INT. INCL.)
10^{-3}
10^{-4}
10^{-5}
10^{-6}
10^{-7}
π^-
Σ^- ($\times 10^2$)
Ξ^- ($\times 10^3$)
Ω^- ($\times 10^4$)
100
110
120
130
140
150
160
170
180
190
200